CHAPTER 6

Effect of Pressure on Fast Side Chain Motions of Ubiquitin

6.1 Introduction

The protein conformational fluctuations between a broad spectrum of conformational basins spanning the natively folded state to unfolded state are necessary for protein-mediated biological functions. The rugged potential energy landscape with mutiple energy minima corresponding to various conformational substates separated by energy barriers gives rise to heterogenous protein dynamics. The atomic fluctuations within and across conformational substates contribute to the vibrational and conformational dynamics of proteins, respectively.[8] Both vibrational and conformational fluctuations of proteins are sensitive to various thermodynamic parameters including temperature and pressure and on environmental factors such as hydration, pH of solvent, ionic strength and ligand binding. The temperature dependence of mean square fluctuations of atoms in proteins obtained using neutron scattering experiments showed a harmonic to anharmonic dynamical transition at around 200K.[81,112,196] The protein-glass transition is observed to be independent of the pressure indicating that the energy barriers separating the harmonic substates are unaltered by pressure. The influence of pressure on the conformational energy landscape of proteins has not been explored much.

The volume, compressibility and both fast and slow motions of proteins are signi cantly altered upon changing the external pressure.[197–200] Various experimental techniques including tryptophan fluorescence and phosphorescence, Fourier transformed infrared (FTIR) spectroscopy, nuclear magnetic resonance (NMR) spectroscopy and X-ray crystallography are

used to probe responses of protein dynamics to pressure perturbations. Upon increasing the pressure, protein fluctuations gradually decrease at moderate pressures (< 2 kbar) while at high pressures (> 2 kbar) proteins denature due to the destabilization of hydrophobic cores. The pressure response and onset denaturation pressure are different (4-10 kbar range or more) for different proteins. For instance, lyzozyme did not exhibit signi cant changes in average volume at 3 kbar while BPTI at 10 kbar exhibited decrease in radius of gyration, backbone fluctuations and compressibility leading to unfolding.[201,202]

The amplitude of atomic fluctuations and volume of proteins increase with increasing temperature whereas they decrease with increase in pressure. The temperature-induced protein unfolding is understood on the basis of transfer of nonpolar (hydrophobic) residues into the water. The pressure-induced unfolding has been attributed to the penetration of water into the hydrophobic core of the protein. The pressure-induced unfolding has been studied well and understood based on the global properties but site-speci c dynamical changes contributing to the unfolding are not well characterized.[203,204] Site-speci c NMR spectroscopy in combination with high-pressure techniques has emerged as a powerful tool to probe the responses of fast internal motions of individual residues in proteins to external pressure. A recent study characterizing the pressure effects on the ps-ns fast internal motions in proteins showed that the side chain dynamics is more sensitive to external pressure than the backbone dynamics.[65]

The present study investigates the influence of pressure on fast internal motions of ubiquitin using molecular dynamics (MD) simulations and free energy calculations performed at 0.001, 0.4, 0.8, 1.2, 1.6, and 2.5 kbar pressures. The side chain conformational free energy pro les were obtained for all methyl-containing residues at all pressures and pressure-induced changes in methyl order parameters, O^2_{axis}, rotamer populations and conformational barriers of individual residues are examined. The degree of pressure-induced perturbations in the free energy pro les and dynamics are different for different residues: a linear O^2_{axis} versus pressure correlation was observed for some residues while the correlation was non-linear for others. The pressure dependence of the correlation between O^2_{axis} and side chain rotamer populations is also examined.

6.2 Simulation Details

Molecular dynamics (MD) simulations are performed on ubiquitin (PDB ID: 1UBQ) using NAMD2.9[101] with CHARMM27 all-atom force- eld.[102] The protein was solvated in a TIP3P water box of dimensions 40Å $\times$ 42Å $\times$ 46Å. The energy of the system was minimized using the conjugate gradient method followed by 3 ns of NPT equilibration MD runs at 300 K temperature and at different pressures (0.01, 0.4, 0.8, 1.2, 1.6, and 2.5 kbar). Subsequently, at each pressure, ve independent 10 ns production runs starting from different initial velocities were performed in the NPT ensemble at 300 K using a Langevin thermostat and a barostat with a damping coef cient of 5 ps^{-1}. Figure 6.1 shows that ubiquitin is maintained at desired pressures throughout the simulations. The equations of motion were integrated with a time step of 1 fs. The nonbonded pair-interaction potential was truncated at 12 Å and smoothed between 10 and 12 Å using a cubic switching function. The periodic boundary conditions were applied along all three dimensions. The electrostatic interactions were computed using the particle mesh Ewald (PME) method[104] with a real space cutoff of 13 Å, and the reciprocal space interactions were computed on grids (using sixth-degree B-splines) of suitable dimensions. The adaptive biasing force (ABF) method was used to accelerate the side chain conformational sampling and to obtain sampling error-free estimates of the side chain conformational free energy landscapes at different pressures with methyl torsional angle, ϕ, as the reaction coordinate (Figure 3.1 of Chapter 3). The mean force as a function of the chosen reaction coordinate was accumulated in bins of width 1° from a total simulation time of 65ns.

6.3 Results and Discussion

6.3.1 Free Energy Pro les

The ϕ-dependent side chain conformational free energy surfaces, F(ϕ), at different pressures are compared with those obtained at ambient pressure. Figure 6.2(a) shows the pressure-induced changes in the side chain conformational energy surfaces of a few representative

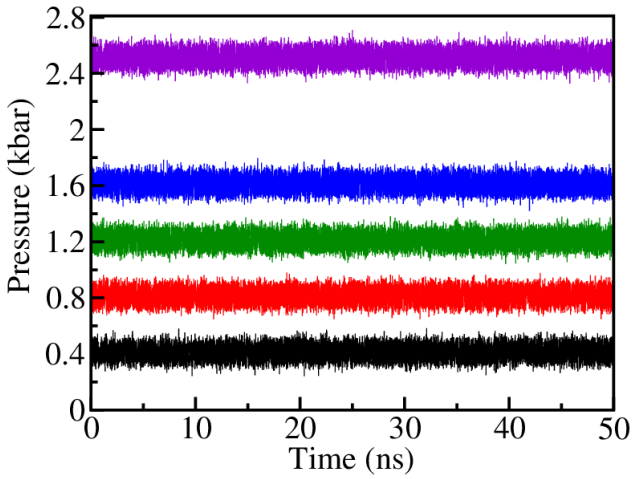

Figure 6.1: Ubiquitin maintained at different pressures during MD simulations.

Table 6.1: Range of the Difference in Free Energy between the Most and Least Stable Side-Chain Conformations (F_{max}).

Residue type	F_{max} (kcal/mol)					
	0.001 kbar	0.4 kbar	0.8 kbar	1.2 kbar	1.6 kbar	2.5 kbar
LEU $^{\delta 1}$	6.66-7.56	6.52-7.50	6.69-7.82	6.54-8.27	6.72-7.56	6.71-7.63
LEU $^{\delta 2}$	6.67-9.05	6.47-8.96	6.29-8.51	6.66-9.15	6.74-8.95	6.54-8.98
ILE $^{\delta}$	6.93-11.42	6.79-10.23	7.06-10	7.67-10.81	7.23-10.84	7.29-10.37
ILE$^{\gamma 2}$	7.62-10.57	7.55-10.75	7.45-10.86	7.84-10.91	7.25-10.97	7.46-9.74
VAL$^{\gamma 1}$	6.91-8.89	7.35-9.05	8.61-9.18	7.88-9.23	8.20-8.94	7.69-9.46
VAL$^{\gamma 2}$	8.08-10.33	7.65-9.89	7.61-10.11	7.68-9.83	7.72-9.79	7.75-10.04
THR$^{\gamma 2}$	8.29-11.50	8.83-11.57	9.07-12.19	8.35-11.69	8.16-12.71	8.51-11.78
MET	5.35	5.57	5.41	5.12	5.57	5.28

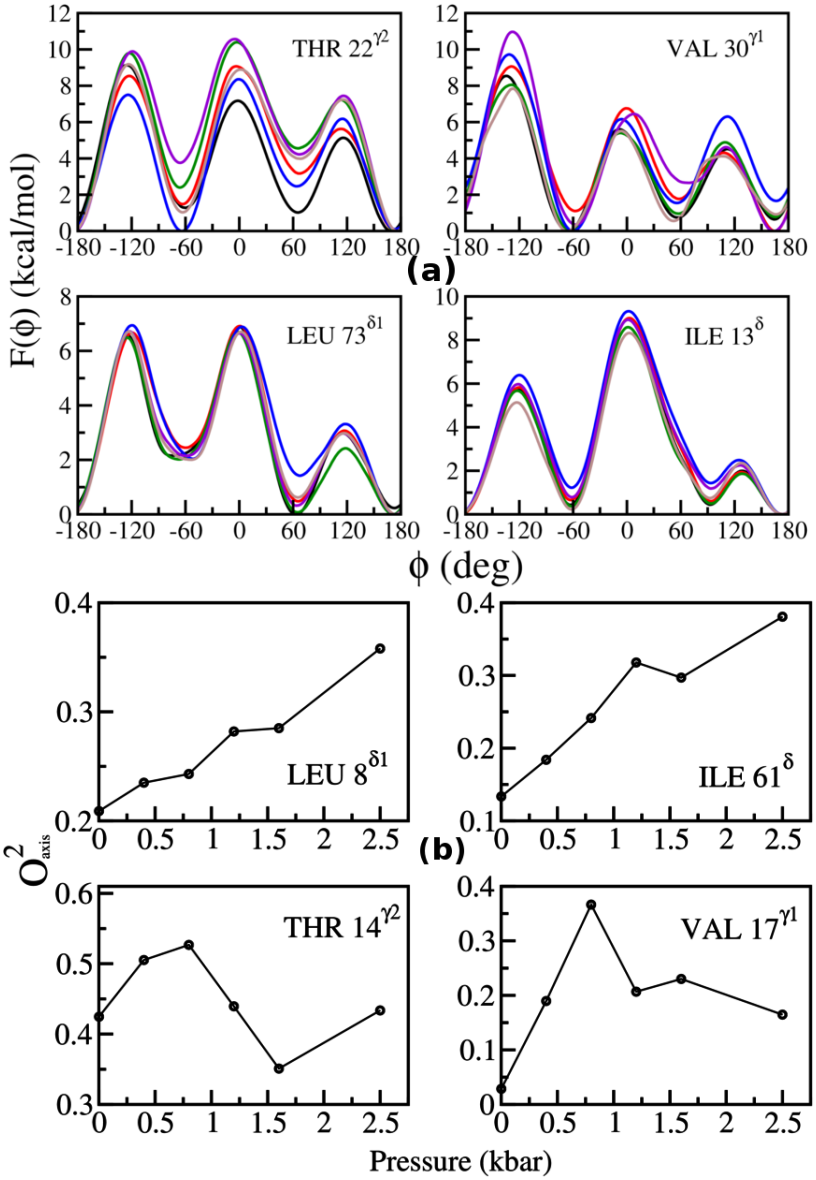

Figure 6.2: (a) Free energy pro les at different pressures (0.001 kbar-black, 0.4 kbar-red, 0.8 kbar-green, 1.2 kbar-blue, 1.6 kbar-violet, 2.5 kbar-violet) and (b) Variation of O^2_{axis} with pressure are shown for few representative methyl-containing residues.

residues.

The difference in free energy between the most and least stable side chain conformations, F_{max}, for different types of residues of ubiquitin at different pressures are shown in Table 6.1. F_{max} is a measure of the extent of conformational restriction experienced by a given side chain. Higher the F_{max} more is the conformational restriction of the side chain. The lower values of F_{max} for MET at all pressures studied indicate that MET side chain have higher conformational flexibility relative to other side chains. Higher values of F_{max} observed for $\gamma-$methyl side chains indicate that the energy barriers surrounding the rotamer states are higher relative to that of $\delta-$methyl side chains. At different pressures, it is found that $\gamma-$methyl side chains (VAL$^{\gamma1,\gamma2}$ and THR $^{\gamma2}$) are conformationally more restricted than $\delta-$methyl side chains (LEU$^{\delta1,\delta2}$, ILE$^{\delta}$).

6.3.2 Pressure Sensitivity of O^2_{axis}

The pressure dependence of O^2_{axis} calculated from F(ϕ) is shown in Figure 6.2(b) for few representative methyl-containing residues of ubiquitin. It is evident from Figure 6.2(b) that the flexibility of the residues can either increase or decrease with pressure with some residues showing linear increase with pressure while others exhibit nonlinear response to pressure. A gradual increase of O^2_{axis} with pressure observed for some residues is due to gradual decrease of side chain flexibility with pressure. The pressure-induced decrease in O^2_{axis} exhibited by some residues suggests that these residues become more flexible under the application of pressure. For instance, O^2_{axis} increases gradually with pressure for LEU 8$^{\delta1}$ and ILE 61$^{\delta}$ while O^2_{axis} of THR 14$^{\gamma2}$ increases with pressure upto 0.8 kbar, decreases between 1 to 1.6 kbar, and again increases with pressure between 1.5 kbar and 2.5 kbar. O^2_{axis} of VAL17$^{\gamma1}$ also increases with pressure upto 0.8 kbar and decreases at higher pressures. The variations in O^2_{axis} versus pressure among different residues can be attributed to the heterogenous response of their micro-environment to external pressure. The observed pressure sensitivity of side chain flexibilities of residues showing both linear and nonlinear response to pressure is consistent with the reported experimental results.[65]

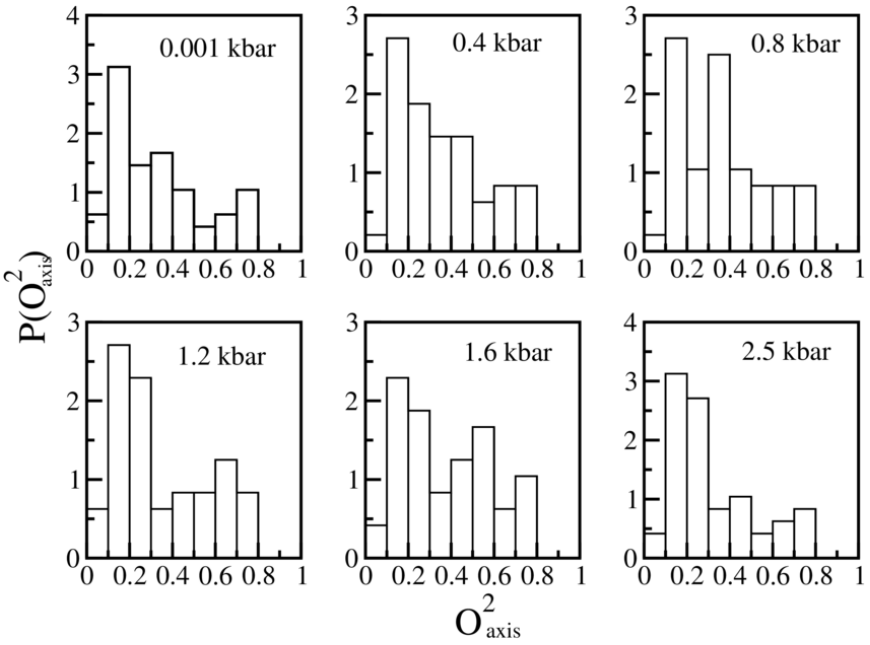

Figure 6.3: Distribution of O^2_{axis} at different pressure for ubiquitin is shown.

6.3.3 Distributions of O^2_{axis}

Figure 6.3 shows the distribution of O^2_{axis} (P(O^2_{axis})) of all methyl-containing residues of ubiquitin at different pressures studied. The broader P(O^2_{axis}) observed indicates the heterogenous nature of side chain motions at all pressures. Pressure induces site-speci c changes in the side chain flexibility of residues evident from the distinct P(O^2_{axis}) at different pressures. P(O^2_{axis}) at 0.001 kbar, 1.6 kbar and 2.5 kbar pressures exhibit trimodal distribution corresponding to three classes of motions referred by NMR relaxation studies as J-class (residues with low O^2_{axis}), ω-class (residues with higher O^2_{axis}) and -class (residues with intermediate O^2_{axis}). The experimental P(O^2_{axis}) are also observed to be different but were almost trimodal at different pressures investigated.[65]

O^2_{axis} versus pressure data for the residues that showed increase in O^2_{axis} with pressure were tted to a straight line to determine the slope, dO^2_{axis}/dp. As changes in O^2_{axis} reflects the changes in the local volume accessible to motion of the side chain, dO^2_{axis}/dp can correspond to the local compressibility of the side chain. The broader distribution of dO^2_{axis}/dp

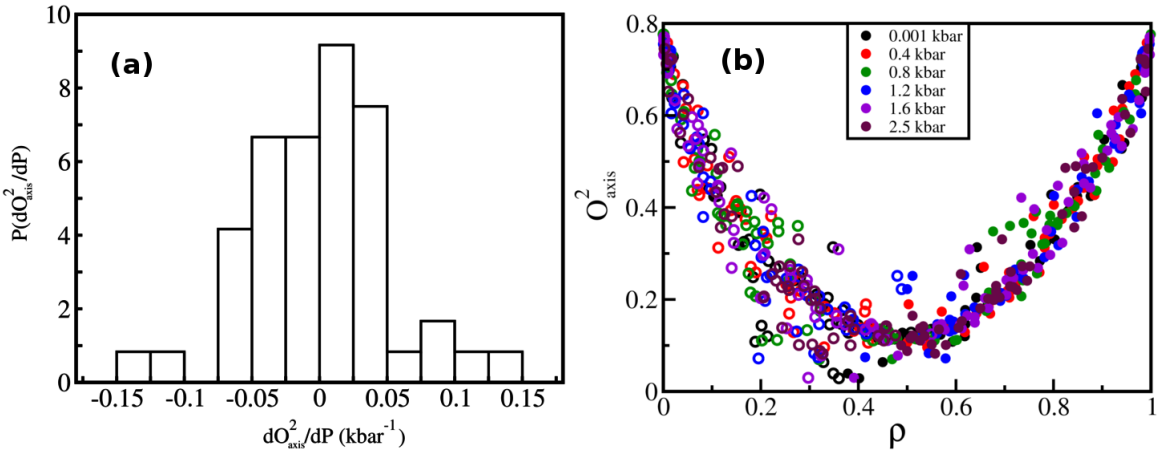

Figure 6.4: (a) Distribution of dO^2_{axis}/dP is shown. (b) Dependence of $O^2_{axis,ABF}$ on the populations of major (ρ_1 - lled circles) and intermediate (ρ_2 - open circles) states color coded for different pressures.

(Figure 6.4(a)) indicates the heterogenous nature of response of side chains to pressure.

6.3.4 Side Chain Flexibility Versus Rotamer Populations at Different Pressures

The populations (ρ) of the major (ρ_1), intermediate (ρ_2), and minor (ρ_3) rotameric states of any given side chain are determined from F(ϕ) using the procedure discussed in Chapter 3. It is observed that O^2_{axis} increases with increasing ρ_1 and decreases with ρ_2 (Figure 6.4(b)) consistent with the universal parabolic correlation between O^2_{axis}, ρ_1 and ρ_2 for many proteins. Though O^2_{axis}, ρ_1, ρ_2 of individual residues change with pressure, the overall parabolic O^2_{axis} versus ρ_1, ρ_2 correlation is retained at all pressures (Figure 6.4(b)) suggesting that the pressure-induced changes in O^2_{axis} and ρ must be governed by this parabolic correlation.

6.3.5 Structural Characterization of Ubiquitin at 2.5 kbar

Figure 6.5 shows the overlay of ubiquitin structures at ambient pressure and at 2.5 kbar. There is a minimal change in the structure of ubiquitin at 2.5 kbar whereas the loop regions deviate signi cantly. The fast side chain motions are perturbed signi cantly at 2.5 kbar pressure but

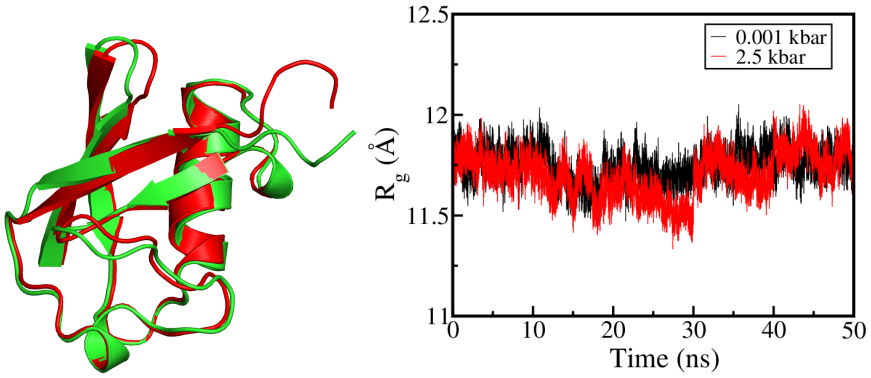

Figure 6.5: (a) Overlay of ribbon representations of ubiquitin structures at ambient pressure (red) and at 2.5 kbar pressure (green) is shown (b) Time evolution of radius of gyration (R_g) of ubiquitin at ambient and 2.5 kbar pressures is shown.

with no large structural variations. This indicates that pressure required for large structural changes and thus for denaturation of ubiquitin is much higher than 2.5 kbar. The variation of radius of gyration of ubiquitin as a function of time at ambient and 2.5 kbar shown in Figure 6.5 has an average value of 11.8Å at both pressures indicating that structure remains intact even at 2.5 kbar.

6.4 Conclusions:

The external perturbations such as binding of ligands, temperature, and pressure can modulate the energy landscape leading to change in protein dynamics and functional activity. The pressure dependence of fast side chain motions in ubiquitin at moderate pressures of range 0.001-2.5 kbar is examined here using MD simulations and free energy methods. O^2_{axis} of all methyl-containing residues showed both linear and nonlinear response to pressure indicating that the side chains can either become more flexible or more rigid upon application of pressure. The broader distribution of the local compressibility of the side chains (dO^2_{axis}/dP) obtained reflects the heterogenous response of side chains to pressure. Though individual residues were observed to respond differently to pressure, the parabolic correlation between O^2_{axis} and conformational population is retained at all pressures studied.